J. Mater. Environ. Sci. 8 (1) (2017) 116-126
ISSN : 2028-2508
CODEN: JMESCN

The roles of 3,4-diamino-5-phenyl-4H-1,2,4-triazole(TR) on the corrosion inhibition of steel in HCl media

Y. EL Bakri*[1], Y. EL Aoufir[2,4], H. Bourazmi[2], A. Harmaoui[1], J. Sebhaoui[1],A. Ben Ali [5], H. Oudda[4], A. Guenbour[2],M. Tabyaoui[2], Y. Ramli[3] and E.M Essassi[1]

[1]*HeterocyclicOrganic Chemistry LaboratoryURAC 21, Facultyof Sciences, Mohammed V University, Rabat, Morocco*
[2]*Materials, Nanotechnology andEnvironmentLaboratory, FacultyofSciences, Rabat, Morocco*
[3]*Medicinal Chemistry Laboratory, Faculty of Medicine and Pharmacy, Mohammed V University, 10170 Rabat, Morocco*
[4] *Separation ProcessesLaboratory, Central Post, Kenitra, Department of Chemistry, Faculty of Sciences, UniversityIbnTofail, Morocco*
[5]*National Laboratory for Drug Control, Al Irfane Rabat Morocco*

Received 18Jun 2016, Revised 24 Oct 2016, Accepted 29 Oct 2016
**For correspondence: Email:youness.chimie14@gmail.com*

Abstract

Inhibiting effect of 3,4-diamino-5-phenyl-4H-1,2,4-triazole(TR) on carbon steel corrosion (CS) in 1M HCl solution was investigated by electrochemical impedance spectroscopy and potentiodynamic polarization measurements at 303-333 K in the presence of different concentrations of inhibitor study ranging from 10^{-3}M to 10^{-6}M. Potentiodynamic polarization study clearly revealed that the compound acted as the mixed type inhibitor. The inhibition efficiency decreases with rising temperature. Impedance measurements showed that the double-layer capacitance decreased and charge-transfer resistance increased with increase in the inhibitor concentration and hence increasing in inhibition efficiency. The results obtained from the different methods are in good agreement. Adsorption followed Langmuir isotherm with negative value of $\Delta G°_{ads}$, suggesting a stable and spontaneous inhibition process.

Keywords: Carbon steel C35, EIS, potentiodynamic polarization, Acid media.

1. Introduction

Ever since its first production roughly 4,000 years ago, iron has played a central role in human society due to its excellent mechanical properties and the abundance of its ores. Today, iron is used in much larger quantities than any other metallic material and is indispensable in infrastructure, transportation, and manufacturing. The steel is widely used in many applications such as desalination plants, construction materials, pharmaceutical industry, and thermal power plant, due to their stability, good corrosion resistance, high strength, workability and weld ability [1-10]. Acid solutions are generally used for the removal of undesirable scale and rust in severalindustrial processes. Hydrochloric and sulphuric acids are widely used in the pickling processes of metals; however, these acids attack the metal and initiate corrosion. This corrosion can cause serious damage to the metal and degrade its properties, thereby limiting its applications [11,12]. One of the most practical methods for protection against corrosion and prevention of unexpected metal dissolution and acid consumption, especially in acidic mediais the use of inhibitors. Different organic and inorganic compounds have been studied as inhibitors to protect metals from corrosive attack. Most of the excellent acid inhibitors are organic compounds containing nitrogen [13-15], oxygen [16-19], phosphorus [20] and sulphur [21-24], because they facilitated its adsorption on the metal surface [25, 26]. Among several categories of triazole compounds, there are the triazole class [27]. The structure of these molecules contains three nitrogen atoms in its penta ring, and is well known as the non-toxic chemicals compounds [26]. For these reasons, they have been the subject of many studies on their ability to act as

corrosion inhibitors for various metals and alloys [26,28-30]. Many researchers have reported the different activities of 4-amino-1, 2,4-triazoles [31,32]. These heterocyclic systems have important industrial, agro-chemical, pharmaceutical and chemical applications [33]. In this contribution, we have investigated the effect of addition of 3,4-diamino-5-phenyl-4H-1,2,4-triazole (TR) on the corrosion inhibition of carbon steel in 1 M HCl medium by electrochemical impedance spectroscopy (EIS) and polarization curves. Adsorption mode and corrosion inhibition mechanism on the carbon steel surface were discussed. Figure 1 shows the molecular structure of the triazole derivative utilised in this investigation.

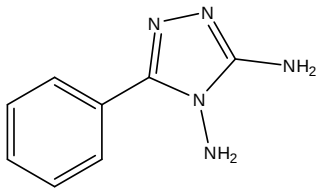

Figure 1: Chemical structure of 3,4-diamino-5-phenyl-4H-1,2,4-triazole (TR)

2. Experimental

2.1.*Solutions and carbon steel samples preparation*

The 1M solution of HCl was prepared by dilution of analytical grade HCl 37% with distilled water. The test solutions were freshly prepared before each experiment by adding inhibitor TRdirectly to the corrosive solution. Concentrations of inhibitor TR were 10^{-3}M to 10^{-6}M.

All studies were carried out using Carbon Steel (CS) sample of composition (Euronorm: C35E carbon steel and US specification: SAE 1035), the steel sample (0.370 % C, 0.230 % Si, 0.680 % Mn, 0.016 % S, 0.077 % Cr, 0.011 % Ti, 0.059 % Ni, 0.009 % Co, 0.160 % Cu and the remainder iron (Fe)) were polished with emery paper up to 1200 grade to obtain very smooth surface, washed thoroughly with double-distilled water, degreased with acetone and dried at room temperature. For electrochemical studies, specimens with an exposed area of $1cm^2$ were used.

2.2.*Synthesis*

Synthesis of 3,4-diamino-5-phenyl-4H-1,2,4-triazole

The required precursor, 3,4-diamino-5-phenyl-4H-1,2,4-triazole were prepared from methyl benzoate which were then converted to aroyl hydrazine by refluxing with hydrazine hydrate in ethanol followed by conversion to aroylthiosemicarbazide on heating with potassium thiocyanate in aqHCl. Aroylthiosemicarbazide were then converted to 5-aryl-1.2.4-thiadiazoles, were then converted to 5-aryl-1.2.4-triazoles by refluxing with hydrazine hydrate in ethanol for 4 hours.

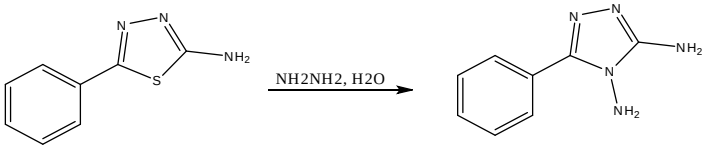

The compound was characterized by N.M.R. ^{1}H-NMR (DMSO-d6) (δ ppm): 6.99(s,2H,NH_2), 5.77(s,2H,NH_2), 8.29(d,1H;CH), 7.51(t,1H,CH) 7.41(t,1H,CH),. ^{13}C-NMR (DMSO-d6) (δ ppm): 155.8(C=N), 129.2(C=C), 151.1(C=C).

2.3.*Electrochemicalmeasurements*

2.3.1 Electrochemicalimpedancespectroscopy

The electrochemical measurements were carried out using VoltaLab (Tacussel- Radiometer PGZ 100) potentiostat and controlled by Tacussel corrosion analysis software model (Voltamaster 4) at under static condition. The corrosion cell used had three electrodes. The reference electrode was a saturated calomel electrode (SCE). A platinum electrode was used as auxiliary electrode of surface area of $1cm^2$. The working electrode was carbon steel. All potentials given in this study were referred to this reference electrode. The working electrode was immersed in test solution for 30 minutes to a establish steady state open circuit potential (E_{ocp}). After measuring the (E_{ocp}), the electrochemical measurements were performed. All electrochemical tests have been performed in aerated solutions at 303 K. The EIS experiments were conducted in the frequency range from high limit of 100 kHz to low limit 0.1 Hz at open circuit potential, with 10 points per decade, at the rest potential, after 30 min of acid immersion.The best semicircle can be fit through the data points in the Nyquist plot using a non-linear least square fit so as to give the intersections with the *x*-axis.
The inhibition efficiency of the inhibitor was calculated from the charge transfer resistance values using the following equation:

$$\eta_Z\% = \frac{R_{ct}^{i} - R_{ct}^{\circ}}{R_{ct}^{i}} \times 100 \qquad (1)$$

Where, R°_{ct} and R^{i}_{ct} are the charge transfer resistance in absence and in presence of inhibitor, respectively.

2.4. *Potentiodynamicpolarization*

The electrochemical behavior of carbon steel sample in inhibited and uninhibited solution was studied by recording anodic and cathodicpotentiodynamic polarization (PDP) curves. Measurements were performed in the 1M HCl solution containing different concentrations of the tested inhibitor by changing the electrode potential automatically from -800 mV to 0 mV versus corrosion potential at a scan rate of 2 mVs^{-1}. The linear Tafel segments of anodic and cathodic curves were extrapolated to corrosion potential to obtain corrosion current densities (i_{corr}). From the polarization curves obtained, the corrosion current (i_{corr}) was calculated by curve fitting using the equation:

$$i = i_{corr}\ [\exp\left(\frac{2.3\Delta E}{\beta_a}\right) - \exp(-\frac{2.3\Delta E}{\beta_c})] \qquad (2)$$

The inhibition efficiency was evaluated from the measured i_{corr} values using the relationship:

$$\eta_{Tafel}\% = \frac{i^{\circ}_{corr} - i^{i}_{corr}}{i^{\circ}_{corr}} \times 100 \qquad (3)$$

Where, i°_{corr} and i^{i}_{corr} are the corrosion current density in absence and presence of inhibitor, respectively.

3.Results and discussion

3.1. *Potentiodynamicpolarization measurements*

The potentiodynamic polarization curves of the CS electrode in 1M HCl obtained with and without various concentrations of used TR (ranging between 10^{-3}M and 10^{-6}M) is presented in Fig.2. Electrochemical parameters such as corrosion current density (i_{corr}), corrosion potential (E_{corr}), Tafel slope constants calculated from Tafelplots ($-\beta_c$), anodic Tafel slope (β_a), the inhibition efficiency ($\eta_{Tafel}\%$), and the degree of surface coverage (θ) were determined by Tafel extrapolation method at all studied concentrations are given in Table 1.

Table 1: Polarization data of CS in 1M HCl without and with addition of TR at 303 K.

Inhibitor	C (M)	E_{corr} (mV/SCE)	i_{corr} (mA cm^{-2})	β_a (mV dec^{-1})	$-\beta_c$ (mV dec^{-1})	η_{Tafel} %	θ
Blank	1M	-477	0.583	101.4	137.8	-	-
TR	10^{-6}	-470	0.357	75.1	68.3	39	0.39
	10^{-5}	-461	0.207	74	50.4	65	0.65
	10^{-4}	-462	0.129	73.1	46.4	78	0.78

	10^{-3}	-483	0.061	58.4	46.5	90	0.90

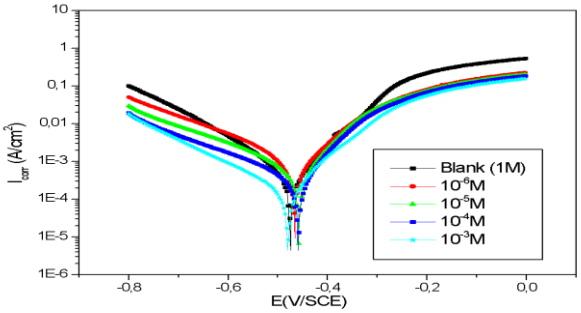

Figure 2: Potentiodynamic polarization curves for carbon steel at 303 K in 1M HCl solution in the absence and the presence of various concentrations of TR.

It is seen that the addition of TR affects the polarization curves and consequently decreases i_{corr}significantly, due to increase in the blocked fraction of electrode surface by adsorption. Cathodic curves gave rise to parallel Tafel lines indicating that the hydrogen evolution is activation controlled and the reduction mechanism is not affected by the presence of inhibitor. These results demonstrated that the hydrogen evolution reaction was inhibited and that the inhibition efficiency increased withincreasing concentration of the inhibitor.
The presence of inhibitor does not cause any significant shift in the E_{corr} values for all concentration. This implies that the inhibitor TR acts as a mixed-type inhibitor, affecting both anodic and cathodic reactions [34]. According to Riggs and coworkers [35], if the displacement in corrosion potential is more than ±85 mV/SCE with respect to the corrosion potential of the blank, the inhibitor can be considered as a cathodic or anodic type, but the maximum displacement in the present case is less than 20 mV/SCE, which indicates that TR is a mixed-type inhibitor.

3.2. *Electrochemical impedance spectroscopy measurements*
Electrochemical impedance spectroscopy (EIS) is an effective method for corrosion studies of metallic materials. The effect of TR concentration on the impedance spectra of carbon steel in 1M HCl solutions at 303 K is recorded in Fig. 4 (Nyquist plots). It is clear to see that the impedance spectra are significantly changed with addition of different TR concentration. From the Nyquist plots, it was also observed that, even the presence of TR does not alter the style of impedance plots, thus indicating the addition of TR does not change the mechanism for the dissolution of carbon steel in 1M HCl solution [36, 37].
The fitted impedance parameters derived from Nyquist diagrams (R_s, R_{ct}, Q and n) and inhibition efficiency are listed in Table 2. Estimates of the margins of error calculated for the parameters are also presented in Table 2. The diagrams are composed of one capacitive loop. The capacitive loop was related to charge-transfer in corrosion process [38]. The impedance spectra are single depressed semicircles, this is often attributed to frequency dispersion as result of the inhomogeneity of structural or interfacial origin, such as those found in adsorption processes [39,40], and the diameter of the semicircle increases with increasing inhibitor concentration.
Results obtained show that R_{ct} increases and C_{dl} tends to decrease with increasing the inhibitor concentration may suggest the formation of a protective layer on the electrode surface. A decrease in the C_{dl} values, which can result from a decrease in the local dielectric constant and/or an increase in the thickness of the electrical double layer, according to the expression of the double layer capacity presented in the Helmotz model by [41]:

$$C_{dl} = \frac{\varepsilon_0 \varepsilon}{\theta} S \qquad (4)$$

Where θ is the thickness of the double layer, S is the area of the electrode, ε_0 is the permittivity of vacuum (8.85 × 10^{-14} F/cm) and ε is the local dielectric constant. This data suggests that the inhibitor acted by adsorption at the metal solution/interface [42]. The Nyquist plots are analyzed in terms of the equivalent circuit composed with a constant phase element (CPE)

The CPE impedance is defined by two values, Q and his described by the equation [43, 44]:

$$Z_{CPE} = Q^{-1}.(i\omega)^{-n} \qquad (5)$$

Where Q(in $\Omega^{-1}cm^{-2}s^{-n}$) is the CPE constant, ω is the angular frequency (rad.s^{-1}), such as $i^2 = -1$ is the imaginary number and n is a CPE exponent which can be used as a gauge of the heterogeneity or roughness of the surface[45, 46].

The CPE behavior can be quantified by plotting the imaginary part of the impedance as a function of frequency in logarithmic coordinates. The parameters associated with capacitive loop (Q, n and R_{ct})were determined by regression of the simple equivalent circuit presented in Fig.4. The regression results are presented in Table 2. In the same table, are also shown the calculated ''double layer capacitance'' values (C_{dl}), using equation [47–49]:

$$C_{dl} = (Q \times R_{ct}^{1-n})^{\frac{1}{n}} \qquad (6)$$

For analysis of the impedance spectra containing a single capacitive semicircle, the standard Randle's circuit is used [50] (Fig. 3). This circuit gives an accurate fit to all experimental impedance data for our compounds. The equivalent circuit is composed of a solution resistance (R_s), charge transfer resistance (R_{ct}) and a constant phase angle (CPE).

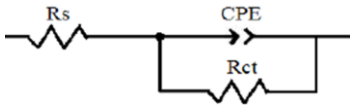

Figure 3: The equivalent circuit model of EIS

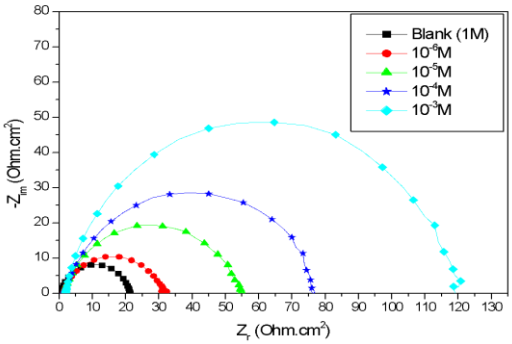

Figure 4: Nyquist diagrams for carbon steel in 1M HCl containing different concentrations of TR at 303K

Table 2: Corrosion parameters obtained by impedance measurements for carbon steel in 1M HCl at various concentrations of TR

	Conc (M)	R_s (Ω cm^2)	R_{ct} (Ω cm^2)	$10^{-4}Q$ ($\Omega^{-1}cm^{-2}s^{-n}$)	N	C_{dl} (μF cm^{-2})	η (%)
Blank	1M	0.54±0.02	20.27±0.44	4.65±0.05	0.80±0.005	149.15	-
	10^{-6}	*1.34* ±0.03	29.5±0.47	3.09± 0.2	0.82±0.009	101.47	32

TR	10^{-5}	1.51±0.03	52.29±0.77	2.42± 0.1	0.83±0.008	81.44	61
	10^{-4}	1.58±0.03	74.51±1.20	1.67±0.09	0.83±0.007	52.09	73
	10^{-3}	1.92±0.03	116±*1*.20	0.87±0.03	0.89±0.005	39.73	83

3.3. *Effect of temperature*

The effect of temperature on the inhibited acid/metal reaction is very complex. Because many changes occur on the metal surface such as rapid etching desorption of inhibitor and the inhibitor itself may undergoes decomposition [51]. To evaluate the adsorption of TR and activation parameters of the corrosion processes of steel in acidic media, polarization measurements are investigated in the absence and presence of inhibitor and also in the range of temperature 303-333 K. The polarization curves of Carbon steel in 1M HCl solution are as shown in Fig.5 in two different conditions, without inhibitor and also in the presence of TR in the temperature range (303-333 K).

The numerical values of the variation of corrosion current density (i_{corr}), corrosion potential (E_{corr}), cathodic Tafel slope (β_c) and anodic Tafel slope (β_a) with the inhibitor at all studied temperatures are given in Table 3.

Close examination of Table 3 shows that an increase in temperature increases i_{corr}. The results also indicate that the inhibition efficiencies decreased with temperature. Such behavior can be interpreted on the basis that the inhibitor acts by adsorbing onto metal surface, and an increase in temperature results in the desorption of some adsorbed inhibitor molecules, leading to a decrease in the inhibition efficiency [52].

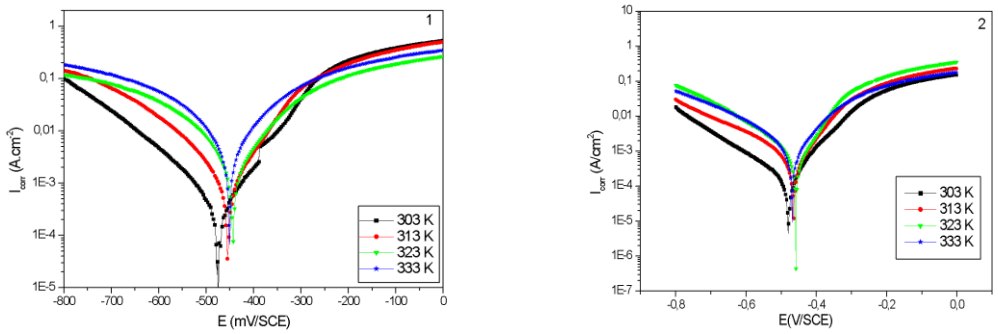

Figure 5: Effect of temperature on the behavior of carbon steel/1M HCl interface in (1) uninhibited solution, (2) at 10^{-3}M of TR.

Table 3: Temperature influence on the PDP parameters for carbon steel in 1M HCl without and withHCl (1M)+10^{-3} M of TR at range temperature 303K-333K.

	Temperature (K)	E_{corr} (mV/SCE)	i_{corr} (mA cm^{-2})	βa (mV dec^{-1})	-βc (mV dec^{-1})	η (%)	Θ
1M HCl	303	-477	0.583	101.4	137.8	-	-
	313	-457.7	0.781	78.7	88.1	-	-
	323	-447.5	0.882	53.5	47.6	-	-
	333	-455.1	0.999	18.6	31.7	-	-
TR	303	-483.2	0.061	58.4	46.5	89.5	0.89
	313	-468.4	0.237	62.1	92.7	70	0.70
	323	-462.6	0.329	61.8	66.1	63	0.63
	333	-472.8	0.473	67.7	72.7	53	0.53

3.4. *Thermodynamic parameters*

The activation energy, enthalpy and entropy of adsorption (E_a, ΔH_a and ΔS_a) can be calculated using the Arrhenius Eq. (7) and transition state Eq.(8) [53]:

$$i_{corr} = Aexp\left(-\frac{E_a}{RT}\right) \quad (7)$$

$$i_{corr} = \frac{RT}{Nh}\exp\left(\frac{\Delta S_a}{R}\right)\exp\left(-\frac{\Delta H_a}{RT}\right) \quad (8)$$

Where E_a is the apparent activation corrosion energy, R is the universal gas constant, A is the Arrhenius pre-exponential factor, h is Plank's constant, N is Avogadro's number, ΔS_a is the entropy of activation and ΔH_a is the enthalpy of activation.

Arrhenius plots for the corrosion rate of carbon steel are given in Fig.6. Values of apparent activation energy of corrosion (E_a) were determined from the slope of ln(i_{corr}) vs. 1/T plots and shown in Table 4. The linear regression coefficient was close to 1, indicating that the carbon steel corrosion in chlorhydric acid can be elucidated using the kinetic model. The calculated value of E_a in the absence of inhibitor (15. kJ mol^{-1}) is in the same order of magnitude as that previously described [54-56].The obtained E_a values in the presence TR is 56.26kJ mol^{-1}.

The increase value of the E_a in presence of inhibitor when compared to that in its absence may be interpreted as physical adsorption [57].

The increase in activation energy can be attributed to an appreciable decrease in the adsorption of the inhibitor on the steel surface with increase in temperature [58].

Fig. 8 shows a plot of ln (i_{corr}/T) vs. 1/T. A straight lines are obtained with a slope of (ΔH_a /R) and an intercept of (ln $(\frac{R}{Nh})$ +$\frac{\Delta S_a}{R}$) from which the values of ΔH_a and ΔS_a are calculated and listed in Table 4. Inspection of these data reveals that the ΔH_a value for dissolution reaction of carbon steel is higher in the presence of TR (ΔH_a=52.97 kJ mol^{-1}) than that in its absence (ΔH_a= 20.80 kJ mol^{-1}). The positive signs of ΔH_a reflect the endothermic nature of the carbon steel dissolution process suggesting that its dissolution is slow in the presence of TR [59]. On comparing the values of the entropy of activation decreases negatively to a greater extent in the presence of TR than in the absence of inhibitor; this reflects the formation of an ordered stable layer of inhibitor on the steel surface [60]. The entropy of activation ΔS_a is more important in the presence of TR than in the absence of inhibitor; this reflects the formation of an disordered stable film of inhibitor on the steel surface.

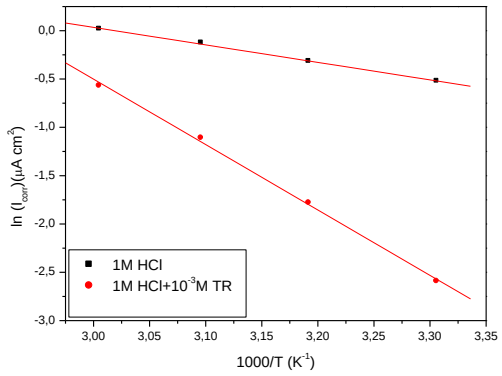

Figure 6: Arrhenius plots for carbon steel i_{corr} in 1 M HCl in absence and in presence 10^{-3} M of TR.

3.5. *Adsorption considerations*

It is well recognized that the first step in inhibition of metallic corrosion is the adsorption of organic inhibitor molecules at the metal/solution interface and that the adsorption depends on the molecule's chemical composition, the temperature and the electrochemical potential at the metal/solution interface. In fact, the solvent H_2O molecules could also adsorb at metal/solution interface. So the adsorption of organic inhibitor

molecules from the aqueous solution can be regarded as a quasi-substitution process between the organic compounds in the aqueous phase [$Org_{(sol)}$] and water molecules at the electrode surface [$H_2O_{(ads)}$] [61]:

$$Org_{(sol)} + xH_2O_{(ads)} \leftrightarrow xH_2O_{(sol)} + Org_{(ads)} \quad (9)$$

where x is the size ratio, that is, the number of water molecules replaced by one organic inhibitor.

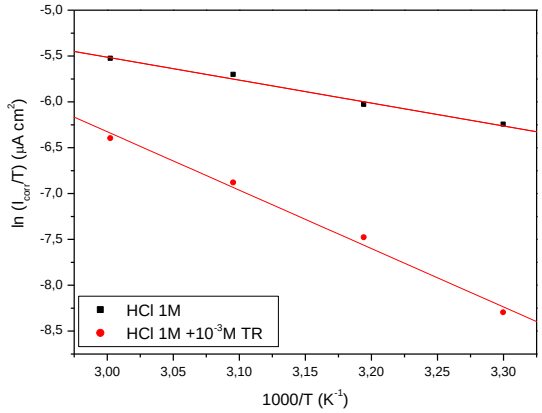

Figure 7: Transition-state plots for carbon steel i_{corr} in 1M HCl in absence and in presence 10^{-3} M of TR.

Table 4: Corrosion kinetic parameters for carbon steel in 1M HCl in absence and presence 10^{-3}M of TR.

Inhibitor	E_a ($KJ.mol^{-1}$)	ΔH ($KJ.mol^{-1}$)	ΔS ($J.mol^{-1}.K^{-1}$)
Blank	15.07	20.80	-180.97
TR	56.26	52.97	-91.21

Basic information on the interaction between the inhibitor and the carbon steel surface can be provided by the adsorption isotherm. In order to obtain the isotherm, the linear relation between degree of surface coverage (θ) values and inhibitor concentration (C_{inh}) must be found. Attempts were made to fit the θ values to various isotherms including Langmuir, Temkin, Frumkin and Flory–Huggins. The best linear relationship was attained using Langmuir adsorption isotherm. This model has also been used for other inhibitor systems [62, 63]. According to this isotherm, θ is related to C_{inh} by:

$$\frac{\theta}{1-\theta} = K_{ads}\, C_{inh} \quad (10)$$

By rearranging this equation:

$$\frac{C_{inh}}{\theta} = \frac{1}{K_{ads}} + C_{inh} \quad (11)$$

Where K_{ads} denotes the equilibrium constant for the adsorption process.

Fig. 8 shows the plots of C_{inh}/θ versus C_{inh} and the expected linear relationship is obtained for all compounds. The strong correlations (R^2 = 0.99982 for the compound TR) confirm the validity of this approach.

The values of K_{ads} obtained from the Langmuir adsorption isotherm are listed in Table 5, together with the values of the Gibbs free energy of adsorption $\Delta G°_{ads}$ calculated from the equation:

$$\Delta G^{\circ}_{ads} = -RT\ln(55.5K_{ads}) \qquad (12)$$

where R is the universal gas constant, T the thermodynamic temperature and the value of 55.5 is the concentration of water in the solution [64].

The value K_{ads} calculated from the reciprocal of intercept of isotherm line is indicating in the Table 5. The high value of the adsorption equilibrium constant reflects the high adsorption ability of this inhibitor on carbon steel surface.

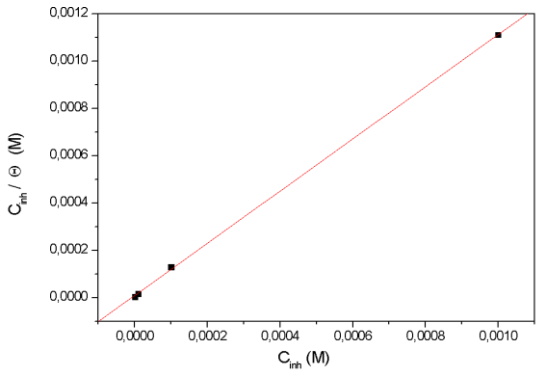

Figure 8: Langmuir adsorption of TR on the carbon steel surface in HCl solution.

Table 5: Thermodynamic parameters for the adsorption of TR in 1M HCl on the carbon steel at 303K**.**

Inhibitor	Slope	K_{ads} (M^{-1})	R^2	$\Delta G°_{ads}$(kJ/mol)
TR	1.10458	0.1330E6	0.99982	-39.84

The negative sign of $\Delta G°_{ads}$demonstrates that the inhibitor is spontaneously adsorbed onto the metal surface. Normally, the magnitude of $\Delta G°_{ads}$ around -20 kJ mol^{-1} or less negative is assumed for electrostatic interactions exist between inhibitor and the charged metal surface (physisorption). Those around -40 kJ mol^{-1} or more negative are indication of charge sharing or transferring from organic species to the metal surface to form a coordinate type of metal bond (chemisorption). The values of $\Delta G°_{ads}$ are between these two, but modestly closer to -40 kJ mol^{-1}. Therefore, it can be interpreted that the adsorption of this inhibitor on the steel surface takes place through both chemical and physical adsorption namely mixed type [65].

Conclusions

The study of 3,4-diamino-5-phenyl-4H-1,2,4-triazole (TR) as a new and effective corrosion inhibitor of CS in 1M HCl solution was conducted using EIS and current–potential measurements. From the results obtained herein, the following points were concluded:

TR exhibits good inhibitive properties for carbon steel (CS) corrosion in 1M HCl solution and the efficiency of inhibition increases with increased inhibitor concentration.

- This inhibitor acted as a mixed-type inhibitor of corrosion by decreasing both cathodic hydrogen reduction reactions and anodic metal dissolution.

- The data obtained from the two different methods PDP and EIS are in good agreement.
- The EIS spectra are described well by relatively simple structural model distributed and therefore modeled by a CPE element.
- The inhibition efficiency decreased with increasing temperature as a result of the higher dissolution of carbon steel at higher temperatures. The addition of TR leads to increase of the activation energy of the corrosion process.
- TR adsorbs according to the Langmuir isotherm model, and the negative value of $\otimes G°_{ads}$ is a sign of spontaneous adsorption on the metal surface.
- The positive signs of ΔH_a reflect the endothermic nature of the carbon steel dissolution process
- The entropy of activation ΔS_a increase in the presence of TR than in the absence of inhibitor; this reflects the formation of an disordered stable layer of inhibitor on the steel surface

References

1. Chen X.Z., Shen Z., Li P., Bruce M., Huang Y. M., Lei Y. C., Huang Q. Y., Zhou J. Z., *Fus. Eng. Design*. 87 (2012) 1569.
2. Brnic J., Turkalj G., Canadija M., Lanc D., Krscanski S., *Mech. Time-Dep. Mat*., 15 (2011) 352.
3. Belfilali I., Chetouani A., Hammouti B., Louhibi S., Aouniti A., Al-Deyab S.S., *Res. Chem. Intermed*, 40 (2014) 1088.
4. Bouhrira K., Chetouani A., Zerouali D., Hammouti B., Yahyi A., Et-Touhami A., YahyaouiR., Touzani R., *Res.Chem.Intermed*, 40 (2014) 586.
5. Ousslim A., Bekkouch K., Chetouani A., Abbaoui E., Hammouti B., Aouniti A., Elidrissi A., Bentiss F., *Res.Chem. Intermed*, 40 (2014) 1221.
6. Belfilali I., Chetouani A., Hammouti B., Aouniti A., Louhibi S., Al-Deyab S.S., *Int. J. Electroch. Sci.,* 7 (2012) 3997.
7. Bouzidi D., Chetouani A., Hammouti B., Kertit S., Taleb M., Al-Deyab S.S, *Int. J. Electrochem. Sci.* 7 (2012) 2334.
8. Chetouani A., Medjahed K., Al-Deyab S S., Hammouti B., Warad I., Mansri A., Aouniti A., *Int. J. Electrochem. Sci*, 7 (2012) 6025.
9. Suraj BA., Deshpande M N., Kolhatkar D G. ,*J. Chem. PharmRes*, 4 (2012) 1035.
10. Chetouani A., Daoudi M., Hammouti B., Ben Hadda T., Benkaddour M., *Corros. Sci*., 48 (2006) 2987.
11. Ji G., Shukla S.K., Dwivedi P., Sundaram S., Prakash R., *Ind. Eng. Chem. Res.* 50 (2011) 11954.
12. Amin M.A., Abd EI-Rehim S.S., EI-Sherbini E.E.F., Bayoumi R.S., *Electrochim. Acta* 52 (2007) 3588.
13. Abd- El-Nabey B. A., Khamis E., Ramadan M. Sh., El-Gindy A., *Corrosion*, 52 (1996) 671.
14. Quraishi M. A., Jamal D., *Corrosion*, 56 (2000) 156.
15. Lagrenee M., Memaru B., Chaibi N., Traisnel M., Vezin H., Bentiss F., *Corros. Sci.*, 43 (2001).
16. Abd El-Rahim S.S., Ibrahim M., Khaled K.F., *J Appl. Electrochem*., 29 (1999) 593.
17. Bentiss F., Traisnel M., Gengembre L., Lagrenee M., *Appl Surf Sci*., 152 (1999) 237.
18. Hosseini M. G., Mertens S.F.L., Ghirbani M., Arshadi M. R., *Mater Chem Phys*., 78 (2003) 800.
19. Migahed M., Mohamed H.M., Al-Sabagh A.M., *Mater Chem Phys*., 80 (2003)169.
20. Khamis E., El-Ashry E. S. H., Ibrahim A.B., *Br Corros J*., 35 (2000) 150.
21. Quraishi M.A., Sharma H. K., *Mater Chem Phys*., 77 (2002) 18.
22. Popova A., Sokolova E., Raicheva S., Christov M., *Corros.Sci*., 45 (2003) 33.
23. Quaraishi M.A., Rawat J., *Mater Chem Phys*., 78 (2002) 43.
24. El Azhar M., Memari B., Traisnel M., Bentiss F., Lagrene'e M., *Corros.Sci.*, 43 (2001) 2229.
25. Kaya S., Tüzün B., Kaya C., BasseyObot I., *J. Taiwan Inst. Chem. Eng.* 58 (2016) 528.
26. Awad M.K., Mustafa M.R., Abo Elnga M.M., *J. Mol. Struct. Theochem*. 959 (2010) 66.
27. Kovacevic N., Kokalj A., *Corros. Sci*. 73 (2013) 7.
28. Soumoue A., El Ibrahimi B., El Issami S., Bazzi L., *IJSR NET* 3 (2012) 349.
29. Mihit M., Bazzi L., Salghi R., Hammouti B., El Issami S., Ait Addi E., *ISJAEE* 62 (2008) 173.
30. El Issami S., Bazzi L., Mihit M., Hammouti B., Kertit S., Ait Addi E., Salghi R., *Pigment. ResinTechnol*. 36 (2007) 161.
31. Tourabi M., Nohair K., Nyasi A., Hammouti B., Jama C., Bentiss F., *J. Mater. Environ. Sci.* 5 (2014) 1133.
32. Bentiss F., Bouanis M., Mernari B., Traisnel M., Lagrenée M., *J. Appl. Electrochem*. 32 (6) (2002) 671.

33. Yadav M., Kumar S., Sinha R.R., Bahadur I., Ebenso E.E., *J. Mol. Liq.* 211 (2015) 135–145.
34. El Ouasif L., Merini I., Zarrok H., El ghoul M., Achour R., Guenbour A., Oudda H., El-Hajjaji F., Hammouti B., *J. Mater. Environ. Sci.* 7 (8) (2016) 2718-2730
35. Riggs O.L. Jr, in Corrosion Inhibitors, ed. by C.C. Nathan (The National Association of Corrosion Engineers (NACE), Houston, 1973), pp. 2.
36. Abd El Rehim S. S., Hassan H. H., Amin M. A., *Mater. Chem. Phys.*, 2002, 337.
37. ElHajjaji F., Greche H., Taleb M., Chetouani A.,, Aouniti A., Hammouti B., *J. Mater. Environ. Sci.* 7 (2016) 566-578.
38. Ashassi-Sorkhabi H., Ghalebsaz-Jeddi N., Hashemzadeh F., Jahani H., *Electrochim. Acta*,51 (2006) 3848.
39. Goncalves R.S., Azambuja D.S., SerpaLucho A.M., *Corros. Sci*., 44 (2002) 467.
40. Bouoidina A., El-Hajjaji F., Chaouch M., Abdellaoui A., Elmsellem H., Rais Z., Filali Baba M., Lahkimi A., Hammouti B. and Taleb M., *Der Pharma Chemica*, 8(13) (2016) 149-157
41. Ghazoui A., Saddik R., Benchat N., Guenbour M., Hammouti B., Al-Deyab S.S., Zarrouk A., *Int. J. Electrochem. Sci*., 2012, 7080.
42. Manssouri M., El Ouadi Y., Znini M., Costa J., Bouyanzer A., Desjobert J-M., Majidi L., *J. Mater. Environ. Sci.* 6 (2015) 631-646
43. Stoynov Z., *Electrochim. Acta* 35 (1990) 1493.
44. Macdonald J.R., *J. Electroanal. Chem.* 223 (1987) 25.
45. Li P., Lin J.Y., Tan K.L., Lee J.Y., *Electrochim. Acta* 42 (1997) 605.
46. Lopez D. A., Simison S.N., de Sanchez S.R., *Electrochim. Acta* 48 (2003) 845.
47. Martinez S., Metikos-Hukovic M., *J. Appl. Electrochem.* 33 (2003) 1137.
48. Wu X., Ma H., Chen S., Xu Z., Sui A., *J. Electrochem. Soc.* 146 (1999) 1853.
49. Ma H., Cheng X., Li G., Chen S., Quan Z., Zhao S., Niu L., *Corros. Sci*. 42 (2000)1669.
50. Achary G., Sachin H.P., ArthobaNaik Y., Venkatesha T.V., *Mater. Chem. Phys.* 107 (2008) 44.
51. Bouanis F.Z., Bentiss F., Traisnel M., Jama C., *Electrochim. Acta*.54 (2009) 2371.
52. Ehteram A. Noor, Aisha H. Al-Moubaraki, *Mater.Chem. Phys.* 110 (2008) 145.
53. BockrisJ.O'M., Reddy A.K.N., Modern Electrochemistry, vol. 2, Plenum Press, New York, 1977.
54. Wang L., Corros. Sci. 48 (2006) 608.
55. Benabdellah M., Aouniti A., Dafali A., Hammouti B., Benkaddour M., Yahyi A., Ettouhami A., *Appl. Surf. Sci*. 252 (2006) 8341.
56. Benabdellah M., Benkaddour M., Hammouti B., Bendahhou M., Aouniti A., *Appl. Surf. Sci*. 252 (2006) 6212.
57. Martinez S., Stern I., *Appl. Surf. Sci.* 199 (2002) 83.
58. Szauer T., Brandt A., *Electrochim. Acta* 26 (1981) 1253.
59. Guan N.M., Xueming L., Fei L., *Mater. Chem. Phys.* 86 (2004) 59.
60. Yurt A., Balaban A., Kandemir S.U., Bereket G., Erk B., *Mater. Chem. Phys.* (2004), 420.
61. Guan N.M., Xueming L., Fei L., *Mater. Chem. Phys.* 86 (2004) 59.
62. Sahin M., Bilgic S., Yılmaz H., *Appl. Surf. Sci.*, 195 (2002) 1.
63. Kissi M., Bouklah M., Hammouti B., Benkaddour B., *Appl. Surf. Sci.*, 252 (2006) 4190.
64. Machnikova E., Whitmire K. H., Hackerman N., *Electrochim. Acta.*, 53 (2008) 6024.
65. Badr G.E., *Corros. Sci.*, 51 (2009) 2529.

(2017) ; http://www.jmaterenvironsci.com/

Mis en forme : Gauche